# Optimizing Altitude Sampling and Sensitivity with the Goldstone Orbital Debris Radar

**James Murray(1), Jessica A. Arnold(2), Alyssa Manis(3), and Mark Matney(3)**

(1) Tomorrow.io, 9 Channel Center St., 7th Floor, Boston, MA 02210, USA; james.murray@tomorrow.io
(2) Jacobs, NASA Johnson Space Center, Mail Code XI5-9E 2101 NASA Parkway, Houston, TX 77058, USA; jessica.a.arnold@nasa.gov
(3) NASA Orbital Debris Program Office, Johnson Space Center, 2101 NASA Pkwy XI511, Houston, TX 77058, USA; alyssa.p.manis@nasa.gov; mark.matney-1@nasa.gov

**Abstract**

The NASA Orbital Debris Program Office (ODPO) has used the Goldstone Orbital Debris radar since 1993 to characterize orbital debris (OD) in LEO too small to be tracked by the U.S. Space Surveillance Network. Operated by NASA's Jet Propulsion Laboratory (JPL), Goldstone can measure OD as small as 3 mm at 1000 km altitude and lower. Goldstone is a bistatic radar that for 25 years used Deep Space Station (DSS)-14 as a transmitter and DSS-15 as a receiver. In early 2018, DSS-15 was decommissioned and replaced with DSS-25 (and occasionally DSS-26) of the Deep Space Network (DSN) Apollo Cluster. The increased baseline between DSS-14 and DSS-25 significantly reduced the instantaneous altitude coverage of the bistatic beam overlap. Initial measurements in 2018 were focused around 800 km, which has approximately the highest flux of sub-centimeter debris. For all of 2019, DSS-14 was taken offline for maintenance, during which time the ODPO developed an annual survey observation plan designed to efficiently sample altitudes from 700 km to 1000 km, since many NASA spacecraft fly in this altitude range. This paper discusses the observation plan, including the development of the pointings, the refinement of the altitudes of interest, and the analysis of the effects of random pointing errors on beam overlap. Additionally, results from measurements taken in 2020–2021 are presented, showing that not only is the observation plan effective at sampling 700 km to 1000 km altitude, but it also produces the most sensitive terrestrial radar measurements at these altitudes to date.

## 1 Introduction

One of the flagship products of the NASA Orbital Debris Program Office (ODPO) is the Orbital Debris Engineering Model (ORDEM). ORDEM is used by spacecraft designers/operators, debris researchers, and mission planners/analysts to estimate the flux of orbital debris (OD) as a function of size, altitude, and inclination for spacecraft and ground-based sensors. To build, verify, and validate these models, the ODPO performs regular measurements of the OD environment. In low Earth orbit (LEO), data for objects larger than approximately 10 cm is obtained from the U.S. Space Surveillance Network (SSN) Satellite Catalog. Data for objects smaller than 1 mm is obtained from *in-situ* measurements, such as the inspection of returned spacecraft surfaces for small object impacts. Terrestrial radar is the primary instrument used for the characterization of centimeter and sub-centimeter sized OD.

The workhorse sensor employed by the ODPO for measurements of centimeter-sized debris in LEO is the Haystack Ultrawideband Satellite Imaging Radar (HUSIR), operated by the Massachusetts Institute of Technology Lincoln Laboratory (MIT/LL) [1]. HUSIR provides data on objects as small as approximately 5 mm at 1000 km altitude. The Goldstone Orbital Debris Radar (Goldstone), operated by NASA's Jet Propulsion Laboratory (JPL), can measure OD as small as 3 mm at 1000 km altitude, making it the most sensitive radar used for these types of measurements. Since particles smaller than 3 mm pose the highest penetration risk to most spacecraft [2], this makes Goldstone a unique and important source of data for OD in this size regime.

For 25 years, OD operations utilized Goldstone's Deep Space Station (DSS) sensors, specifically DSS-14 as a transmitter and DSS-15 as a receiver, to provide a short baseline for beam overlap for all of LEO with a single pointing geometry. In early 2018, DSS-15 was decommissioned and replaced with DSS-25 (and occasionally DSS-26) of the Deep Space Network Apollo Cluster. This increased the bistatic baseline and significantly reduced the instantaneous bistatic beam overlap, requiring altitudes of interest to be targeted [3].

Following this change, the ODPO designed a new annual survey observation plan to optimize the altitude sampling and sensitivity of the new configuration, with the first observations taking place in 2020. This paper discusses the new observation plan, including the development of the pointings, the refinement of the altitudes of interest, and the analysis of the effects of random pointing errors on beam overlap. Results from measurements taken in 2020–2021 are presented, showing that not only is the observation plan effective at sampling 700 km to 1000 km altitude, but it also produces the most sensitive terrestrial radar measurements at these altitudes to date.

## 2 The Goldstone Orbital Debris Radar

The Goldstone Orbital Debris Radar is a bistatic radar in the Mojave Desert near Barstow, California, and is part of the Goldstone Deep Space Communications Complex (GDSCC). The ODPO uses three of the GDSCC antennas for OD data collection; DSS-14 as the transmitter and DSS-25 or DSS-26 as the receiver. Physical dimensions and geographical locations of the antennas are found in [4]. Table 1 lists the nominal operating parameters of the radar system hardware.

Table 1. Radar System Hardware Nominal Operating Parameters

| Operating Parameter | Goldstone |
|---|---|
| Peak Power (kW) | 440 |
| Transmitter Frequency (GHz) | 8.56 |
| Transmitter Wavelength (cm) | 3.5 |
| Transmitter Antenna Diameter (meter) | 70.0 |
| Receiver Antenna Diameter (meter) | 34.0 |
| Transmitter Half Power Beam Width (HPBw) (deg) | 0.03 |
| Receiver HPBw (deg) | 0.06 |
| Transmitter Antenna Gain (dB) | 74.24 |
| Receiver Antenna Gain (dB) | 68.42 |
| Avg. System Temperature (K) | 21.79 |
| Intermediate Frequency Bandwidth (MHz) | 1.5 |

The Goldstone waveform is a linear frequency modulated (LFM) "chirp" with a center frequency of 8.56 GHz and a chirp bandwidth of 300 kHz. Goldstone alternates between positive frequency sloped "up-chirps" and negative frequency sloped "down-chirps." Measurements from pairs of up- and down-chirps are used to mitigate frequency-dependent range biases caused by delay-Doppler (or range-Doppler) coupling effects inherent to LFM waveforms [5]. In May 2021, JPL updated the chirp and receive window parameters of its waveform. Since the beam overlap with DSS-25 and DSS-26 is much smaller than the legacy DSS-15 configuration and such a large unambiguous range is no longer necessary, the pulse period was decreased from 22.503 ms to 18 ms. The chirp duration was also increased from 2.34 ms to 2.9 ms. The net effect of the two changes resulted in a 55% increase in average power (product of peak power and duty cycle).

For OD observations, Goldstone does not track but operates in a beam park mode in which the transmitter is pointed at a fixed azimuth and elevation, the receiver is pointed to intersect the transmitter beam at a target slant range, and objects are detected as they fly through the common volume of the transmitter and receiver beams. For all geometries, the transmitter is pointed at 75° elevation due East (75E), which mimics the primary observation geometry of the HUSIR radar. The receiver, either DSS-25 or DSS-26, is then pointed such that the antenna beams intersect at the altitude of interest. The 75E geometry allows the measurement of range-rates that provide useful estimates of orbital inclination, with a circular orbit approximation, while limiting the additional atmospheric and free space path losses of lower elevation pointings. As part of the development of the new pointing plan, it was determined that the range from 700 km to 1000 km altitude could be effectively covered with only four separate pointings, called A, B, C, and D, with minimal impact to sensitivity at the overlap of adjacent pointings. Figure 1 shows the altitude coverage of the A, B, C, and D pointings, as well as that of the legacy configuration in which DSS-15 was used as a receiver. Details of the development of these pointings are given in Section 3. An overview of results from 2020 to 2021 using this pointing plan are presented in Section 4.

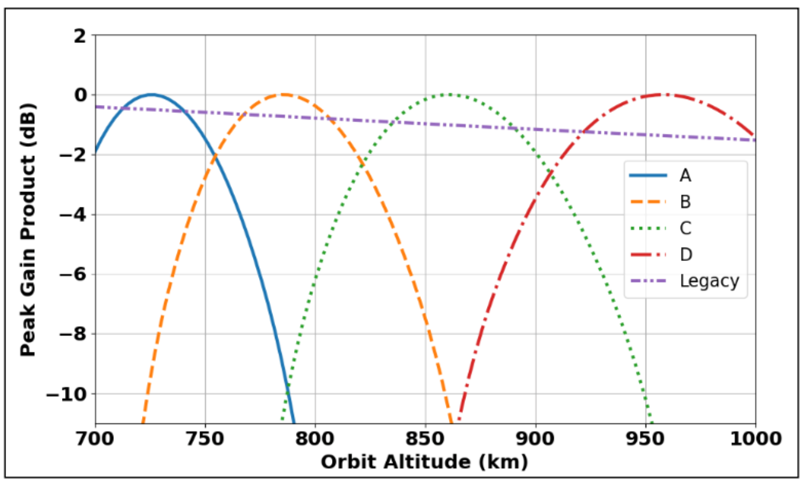


Fig. 1. Peak gain product versus orbit altitude of the A, B, C, D, and legacy pointings showing the extent of their bistatic beam overlaps.

## 3 Development of the Annual Survey Observation Plan

In early 2018, the legacy receiver of Goldstone, DSS-15, was decommissioned. With a relatively short baseline of 500 meters, the legacy Goldstone configuration was able to observe all of LEO with a single pointing. DSS-25 and DSS-26 were identified as replacement receivers, with the drawback of having a longer baseline of approximately 10 km that severely reduces the instantaneous altitude overlap of the transmitter and receiver beams. In 2018, observations with the new geometry primarily used a single pointing with a roughly 100-km altitude extent centered on 800 km. This altitude was chosen because it corresponds to the altitude regime with the highest flux of sub-centimeter-sized OD. Detailed results of these measurements are in [6]. During 2019 and most of 2020, DSS-14 was taken offline for maintenance, giving the ODPO the opportunity to develop a new observation plan optimized for the new bistatic geometry. The main constraints to consider included the number of observations available per year, the altitude regimes of interest, the altitude coverage of an individual pointing, and the loss of sensitivity relative to the legacy Goldstone system.

Goldstone typically collects data in long observation blocks, or tracks, approximately 4 to 8 hours long. To obtain reasonable uncertainties in the measured flux, three observations (about 13 hours) per pointing were necessary. Since Goldstone collects data for the ODPO on an as available basis it was necessary to identify the expected number of tracks and hours of observation from Goldstone in a single year. From 2008 to 2018, an average of 12 tracks (69.2 hours) were collected per year. This limited the number of pointings for an annual survey to four pointings or less to obtain statistically significant data.

### 3.1 Complete LEO Coverage Geometries (400 km – 2000 km)

The short baseline of the historical pairing of DSS-14/DSS-15 (about 500 meters), previously allowed Goldstone to sample all LEO altitudes with a single pointing. To determine the number of pointings required by the new geometry to replicate this ability, the altitude coverage of a single pointing relative to a constant dB gain offset in the previous baseline's peak gain as a function of altitude was defined. Offsets of 6 dB, 3 dB, and 1 dB were chosen for investigation. A reference offset of 6 dB requires 13 pointings, a reference offset of 3 dB requires 18 pointings, and a reference offset of 1 dB requires 29 pointings to cover altitudes from 400 km to 2000 km. Figure 2 shows the results for the 6 dB case. The broad sweeping curve represents the altitude coverage of the legacy pointing. As the intersection altitude decreases, the altitude coverage of each pointing decreases, rapidly increasing the number of pointings needed to cover lower altitudes.

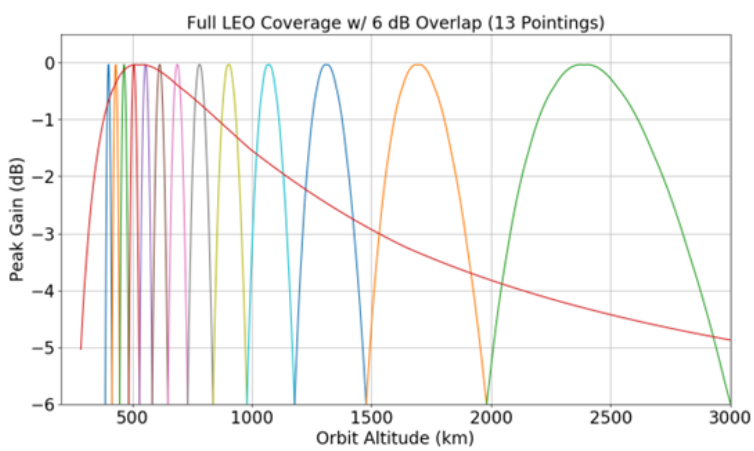


Fig. 2. Peak gain versus orbit altitude showing the number of pointings needed to cover all of LEO where the altitude coverage of a single pointing is defined by a constant offset in peak gain of 6 dB. The broad curve represents the peak gain of the legacy pointing.

Practical constraints on the number of hours obtainable each year and those needed at each pointing to produce statistically significant data make it impossible to survey all of LEO within a single year. Instead, an approach that focuses on altitudes with a higher priority for observations is needed.

### 3.2 Reducing Elevation to Increase Altitude Coverage

One approach to increase the altitude coverage of a single pointing around a particular altitude is to reduce the elevation angle of observation. The increased slant range results in a wider beam of both the transmitter and receiver for a given altitude. Figure 3 shows the widening of the altitude coverage as the elevation angle of the transmitter is reduced at a target altitude of 400 km. When considering the reduced sensitivity due to increased free space path loss (FSPL) at a given altitude, the increased altitude coverage is dwarfed by the loss of sensitivity. By 45° elevation, Goldstone would be no more sensitive than HUSIR (represented by the dashed black line) with a less than 50 km increase in altitude coverage, so reducing the elevation of observation is not a viable method of increasing the altitude coverage of a particular pointing.

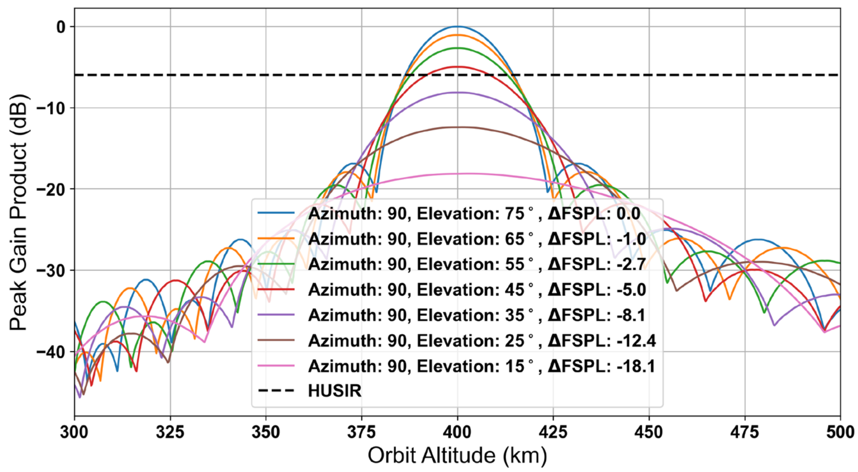


Fig. 3. Peak gain curves centered at 400 km altitude for various transmitter elevations with FSPL relative to 75E included. The dashed black line represents the peak gain product of HUSIR, for comparison.

### 3.3 South Staring Versus East Staring to Increase Altitude Coverage

Another approach to increase altitude coverage of the beam overlap is to aim the antennas along the baseline connecting them, sometimes referred to as “over the shoulder.” Since DSS-25 and DSS-26 lie mostly south of DSS-14, the difference in altitude coverage between a south-pointing and east-pointing geometry was investigated. Figure 4 shows the altitude coverage of east and south pointings at 400 km for an elevation of 75°. Although the altitude coverage is increased, it is negligible. Additionally, the ability to resolve the ambiguity in Doppler inclinations for orbits with inclinations above 90° would be lost, a limitation of Doppler inclination estimation, making this option undesirable.

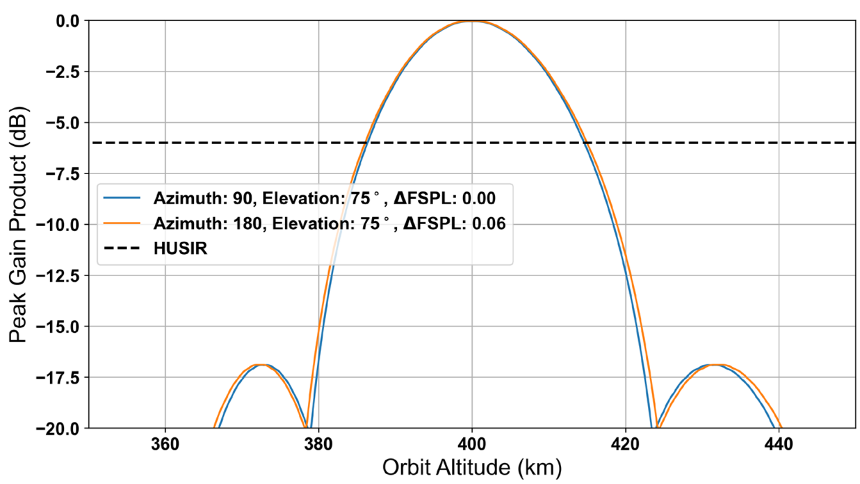


Fig. 4. Peak gain curves centered at 400 km altitude for east- and south-staring pointings at 75° elevation. The dashed black line represents the peak gain product of HUSIR, for comparison.

### 3.4 Limited Coverage Geometry: 700 km – 1000 km

Based on the average observation trends from 2008 to 2018, the maximum number of pointings that can be employed in an observation plan designed for an annual survey is four. Since results show that full LEO coverage (400 km to 2000 km) requires at least 13 pointings, a limited coverage geometry plan was developed to focus on altitudes of interest, namely 700 km to 1000 km. Because the altitude coverage increase from reducing the transmitter elevation was shown to be negligible, it was determined that the optimal pointing for the transmitter, DSS-14, is 75E. This plan was developed assuming the transmitter is pointed 75E, and the receiver pointing is chosen to intersect the transmitter boresight at altitudes of interest.

To determine the altitude coverage of a particular pointing, some convention for when the altitude coverage of a pointing starts and ends must be used. The method used for the full LEO coverage case was to define some fixed gain offset, such as 6 dB, 3 dB, or 1 dB, to determine the start and stop altitudes. To mimic the historical sensitivity of the DSS-14/DSS-15 pair, the convention chosen for the limited altitude coverage analysis was to define the start and stop altitudes in reference to the historical peak gain curve, offset by some constant value. This ensured that the sensitivity of the new geometry was at least as good as the historical geometry at any given altitude. Although the ideal case would have no offset from the historical peak gain curve, analysis showed this would require at least seven individual pointings to cover 700 km to 1000 km. By using an offset of 1.5 dB from the historical peak gain curve, 700 km to 1000 km could be covered with only four pointings and 700 km to 900 km with just three, as shown in Fig. 5. This set of pointings, called A, B, C, and D, were chosen for initial testing.

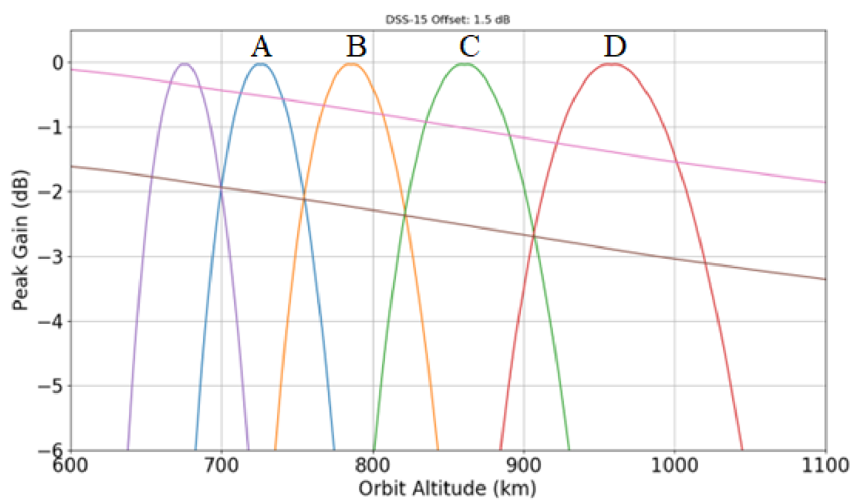


Fig. 5. Pointings needed to cover 700 km to 1000 km in altitude, where the altitude coverage of a single pointing is defined by its intersection with the historical peak gain curve with a 1.5 dB offset, represented by the brown curve. The historical peak gain curve with no offset is represented by the pink curve.

### 3.5 Pointing Error Gain Loss

With the longer baseline, errors in the pointing of the two dishes can have a large effect on the sensitivity. The beams may not align, causing a loss of peak gain. Monte Carlo simulations were performed in which random errors, drawn from Gaussian distributions, were added to the nominal azimuth and elevation of the transmitter and receiver. Based on information received from Goldstone antenna calibration engineers, the maximum standard deviation of cross-elevation ($XEL$) pointing error measured over March to December 2018 was 4.36 millidegrees. As a conservative estimate, this value was used for the standard deviations of the elevation error and cross-elevation error distributions.

The Monte Carlo program accepts inputs for elevation and azimuth for each antenna. The elevation and azimuth for a drawn elevation error, $\Delta EL$, and cross-elevation error, $\Delta XEL$, are given by Eqs. 1 and 2, where $EL_{nominal}$ and $AZ_{nominal}$ are the nominal elevation and azimuth for a given pointing.

$$EL = EL_{nominal} + \Delta EL \quad (1)$$

$$AZ = AZ_{nominal} + \frac{\Delta XEL}{\cos EL_{nominal}} \quad (2)$$

The peak gain product as a function of range was calculated using the perturbed pointings of both the transmitter and the receiver. From this curve, the maximum peak gain product was recorded. This process was then repeated for a total of 10,000 samples, for each transmitter/receiver pair, for each of the four pointings; eight total combinations. Figure 6 shows the resulting distribution of peak gain loss for pointing A using DSS-25 as a receiver. Over 90% of the trials resulted in a loss of less than 0.2 dB. Results for all pointing and receiver combinations were qualitatively similar indicating that the effect on the final RCS/size estimates from Goldstone were small.

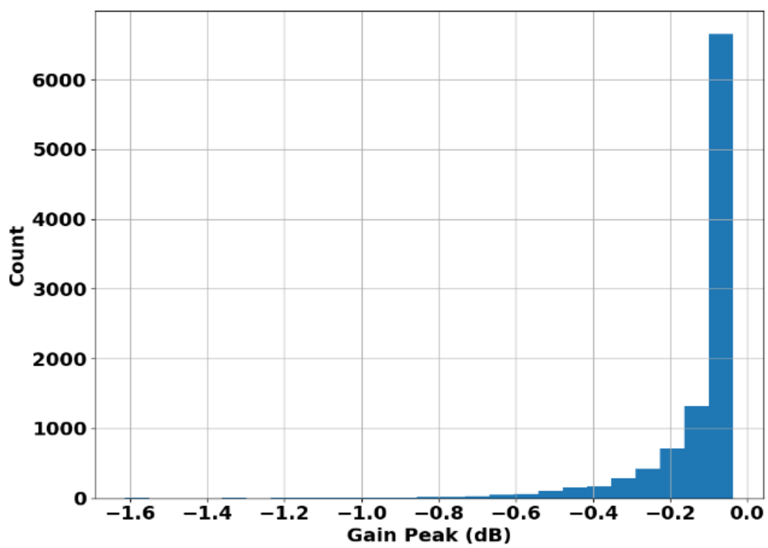


Fig. 6. Distribution of peak gain loss (dB) due to pointing error using DSS-25 as a receiver in pointing A.

## 4 Results From 2020 to 2021

After DSS-14 was brought back online in late 2020, observations were performed using the newly developed pointing plan. From 2020 to 2021, Goldstone performed 102 hours of observations. Due to a hardware issue encountered during this time, data quality control procedures culled the dataset to 30 usable hours. The cause of the issue has since been identified and corrected; re-analysis of the data is underway to recover the affected observations. Additional details and a more detailed description of the data processing and results are found in [7]. Table 2 shows the number of hours, detections, and average count rates for each pointing.

Table 2. Total Number of Hours, Detections, and Count Rate for the Different Pointings Used in CY2020–2021 Data Collection

| Pointing | Number of Hours | Total # of detections | Count Rate (#/hr) |
|---|---|---|---|
| A | 4.2 | 99 | 23.4 |
| B | 10.2 | 268 | 26.2 |
| C | 2.7 | 68 | 25.6 |
| D | 12.9 | 366 | 28.4 |
| **Total** | **30.0** | **801** | **26.71** |

The fundamental measurements made by the radar are range, range-rate, and received power from which radar cross-section (RCS) can be calculated. A circular orbit approximation applied to range and range-rate, or Doppler velocity, can be used to estimate an object's altitude and orbital inclination. Inclinations calculated in this way are referred to as Doppler inclinations. OD size can be estimated from the measured RCS using NASA's Size Estimation Model (SEM) [8].

Figure 7 shows the orbit altitude versus Doppler inclination for objects measured by Goldstone in 2020–2021 at all pointings. When viewed in this way, several on-orbit families of OD become apparent. A large population of debris groups around the vertical dashed black line that indicates the sun-synchronous condition for circular orbits. Several notable on-orbit fragmentation events are highlighted with a black circle, the center of which corresponds to the altitude and inclination of the parent bodies at the time of the event. Additionally, a black ellipse indicates detections associated with the Starlink satellite constellation. This feature has become prominent in both Goldstone and HUSIR datasets. The red horizontal dashed lines indicate the lower and upper bounds of the 700 km to 1000 km altitude of interest.

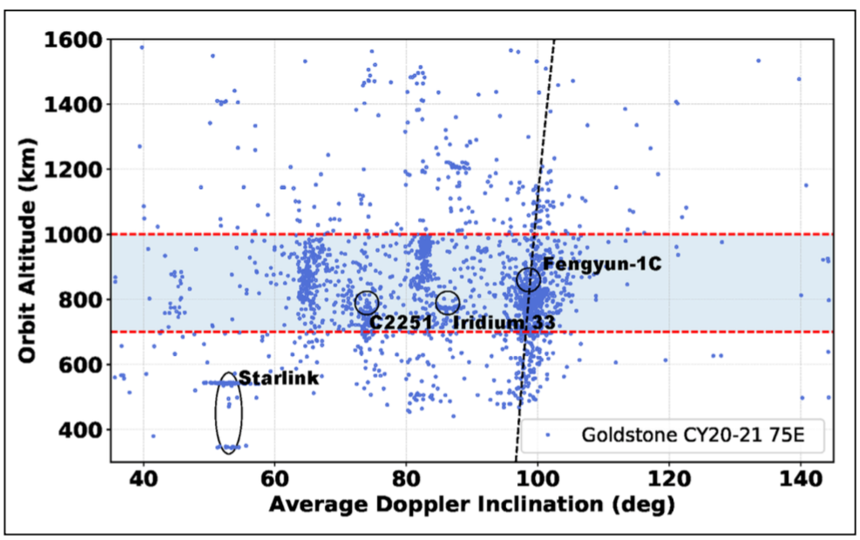


Fig. 7. Orbit altitude versus Doppler inclination, measured by Goldstone in 2020–2021 with the Fengyun-1C and Iridium 33 /Cosmos 2251 (C2251) fragmentation events as well as the Starlink constellation noted by black circles and an ellipse, respectively.

Figure 8 shows the SEM estimated size versus altitude of objects measured by Goldstone in 2020–2021 with all pointings. The red horizontal dashed lines indicate the lower and upper bounds of the 700 km to

1000 km altitude of interest. Detection efficiency decreases rapidly outside of this range, with most detections corresponding to objects large enough to be detected through one or more sidelobes. The dashed black line indicates the altitude dependent size to which the 2020 to 2021 dataset is estimated to be 99% complete; 99% of objects passing through the beam are detected. For comparison, a similar completeness curve for data collected in 2016 using the legacy configuration with DSS-15 as a receiver is shown. An increase in sensitivity that comes from the beam intersection of the pointings in the new plan focuses on these altitudes, whereas the beam intersection of the legacy configuration occurred at 550 km. Adjustments to the transmit duty cycle also contribute to the increased sensitivity. The net effect of the two factors is the improvement of the completeness size from 2.7 mm at 1000 km altitude in 2016 down to 2.2 mm at 1000 km in 2020–2021. These are the most sensitive measurements of OD in LEO made with terrestrial radar to date.

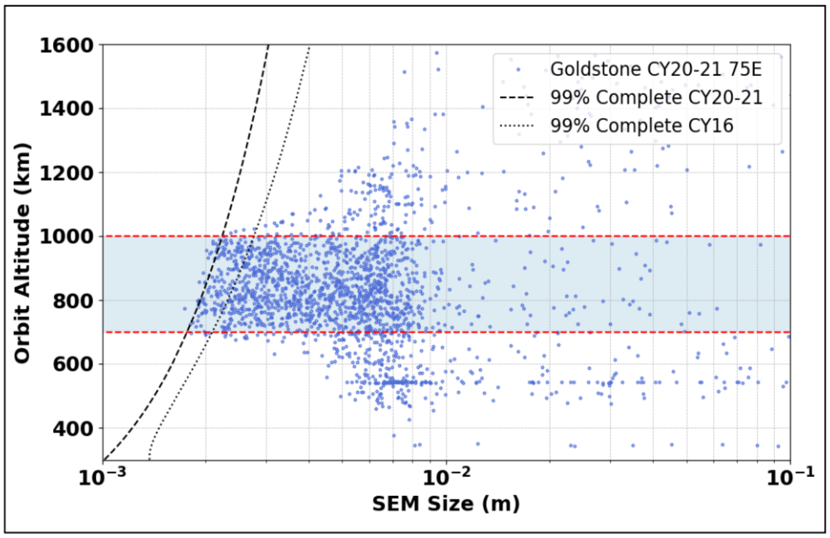


Fig. 8. Orbit altitude versus SEM-size, measured by Goldstone in 2020–2021.

## 5 Conclusion

In this paper, we have presented a comprehensive analysis of the optimization efforts undertaken by ODPO to enhance the altitude sampling and sensitivity of Goldstone. With the transition from the legacy configuration to the new DSS-25 and DSS-26 receivers, challenges arose due to the increased bistatic baseline, resulting in reduced instantaneous altitude coverage. This necessitated the development of a new observation plan tailored to efficiently sample altitudes ranging from 700 km to 1000 km. With rigorous analysis of potential observation geometries and refinement of altitudes of interest, the observation plan successfully addressed these challenges. The four designated pointings (A, B, C, and D) allow effective coverage of a critical altitude range while minimizing sensitivity loss at the overlap of adjacent pointings. The results obtained from Goldstone's observations in 2020–2021 have validated the effectiveness of the observation plan and have demonstrated that it produces the most sensitive terrestrial radar measurements at altitudes between 700 km and 1000 km to date.

## 6 References


1. Murray, J. and Matney, M. "Haystack Ultra-Wideband Satellite Imaging Radar Measurements of the Orbital Debris Environment: 2021," NASA/TP-20230008344, NASA/JSC, Houston, 2023.
2. Squire, M., *et al*. "Joint Polar Satellite System (JPSS) Micrometeoroid and Orbital Debris (MMOD) Assessment," NASA/TM-20150017054, NASA/LRC, Hampton, 2015.
3. Murray, J. "A New Geometry for Debris Observations using the Goldstone Orbital Debris Radar," Orbital Debris Quarterly News, vol. 23, no. 2&3, p. 8, 2019.
4. Slobin, S.D. "DSN Coverage and Geometry," DSN Handbook, 810-005301, Rev. L, 2018.
5. Lee, C., *et al*. "Micro-Meteoroid and Orbital Debris Radar from Goldstone Radar Observations," proceedings of the First International Orbital Debris Conference, ntrs.nasa.gov/citations/20210015979.
6. Miller, R., Murray, J., and Kennedy, T. "Goldstone Radar Measurements of the Orbital Debris Environment: 2018," NASA/TP-20210015780, 2021.
7. J. Murray and M. Matney, “Goldstone Radar Measurements of the Orbital Debris Environment: 2020-2021,” NASA Technical Publication, in-work.
8. Xu, Y.-l. and Stokely, C. "A Statistical Size Estimation Model for Haystack and HAX Radar Detections," in 56th International Astronautical Congress, Fukuoka, Japan, 2005.